Synthesis and Characterization of Tin Niobates

L. P. Cruz,*,† J.-M. Savariault,‡ J. Rocha,* J.-C. Jumas,§ and J. D. Pedrosa de Jesus*

*Department of Chemistry, University of Aveiro, 3810 Aveiro, Portugal; †Department of Environment, Polytechnique Institute of Viseu, 3510 Viseu, Portugal; ‡Centre d'Elaboration de Materiaux et d'Etudes Structurales, CNRS B.P. 4347, Toulouse, France; and §Laboratoire des Agrégats Moléculaires et Matériaux Inorganiques (ESA 5072 CNRS), Université Montpellier II, Place Eugène Bataillon, CC 015, 34095 Montpellier cedex 5, France

The synthesis and the structural characterization of tin niobates $Sn_{1+x}Nb_2O_{6+x}$, $x = 0.0$, 0.5, and 1.0, are reported. The materials have been characterized by bulk chemical analysis, single-crystal and powder X-ray diffraction, and ^{119}Sn Mössbauer and ^{93}Nb and ^{119}Sn solid-state NMR spectroscopies. $SnNb_2O_6$ is a synthetic analog of the rare mineral foordite. Red $Sn_2Nb_2O_7$ crystallizes in a pyrochlore structure with $a = 10.5386$ Å. ^{119}Sn Mössbauer reveals the presence of both Sn(II) and Sn(IV) in pyrochlore samples. ^{119}Sn MAS NMR spectroscopy supports the presence in synthetic foordite of Sn(II) in eight-fold coordination. The six-coordinated Sn(IV) and eight-coordinated Sn(II) ^{119}Sn MAS NMR resonances are not resolved in the $Sn_2Nb_2O_7$ pyrochlore spectrum. ^{93}Nb NMR indicates a fairly distorted local environment for niobium in synthetic foordite, much more so than in the $Sn_2Nb_2O_7$ pyrochlore. © 2001 Academic Press

Key Words: oxides; pyrochlore; tin niobate; crystal structure; ^{119}Sn and ^{93}Nb NMR; ^{119}Sn Mössbauer.

INTRODUCTION

Pyrochlores have been raising considerable interest particularly after the work of Cook and Jaffe reporting that noncentrosymmetric $Ca_2Nb_2O_7$ exhibits important ferroelectric properties and a spontaneous polarisation, variable with the electric field (1, 2). Among all known solids possessing the pyrochlore structure those containing lead are probably the best ferroelectric materials. However, the industrial use of lead poses considerable environmental problems and, thus, it is of interest to replace it by a less toxic element. Because some of the most important properties of pyrochlore Pb(II) materials arise due to the presence of a free electron pair (3) we have attempted to replace lead with tin. Several lead niobates with the pyrochlore structure and formula $Pb_xNb_2O_{6+x}$ ($1 < x < 2$) are known (4), while only two tin niobates, $SnNb_2O_6$ and $Sn_2Nb_2O_7$, have been reported.

Foordite ($Sn^{II}Nb_2O_6$) is a rare mineral first found near Lutsiro, Sebaya River, Rwanda, isostructural with its Ta-rich analog, thoreaulite ($Sn^{II}Ta_2O_6$) (5). At room temperature, foordite does not possess the pyrochlore structure.

The unit cell is monoclinic, space group $C2/c$, with $a = 17.093$, $b = 4.877$, and $c = 5.558$ Å and $\beta = 90.85°$. The structure consists of alternations of two types of layers perpendicular to X (Fig. 1a) (6). One type of layer consists of corner-sharing NbO_6 octahedra forming a flat, perforated, two-octahedron-thick sheet with closed-packed anions. The other layer type consists of distorted edge-sharing $Sn^{II}O_8$ square antiprisms forming a flat, perforated sheet. The Sn(II) coordination polyhedron is much distorted due to the presence of a stereoactive lone electron pair (Fig. 1b) (6). Birchall and Sleight reported a detailed study on non-stoichiometric phases in the Sn–Nb–O and Sn–Ta–O systems having pyrochlore structures (7). In particular, they have discussed the room temperature structure of $Sn_2Nb_2O_7$ and concluded that a significant amount of Sn(IV) is in a fairly symmetric environment (site 16, where niobium also resides). However, this work relied only on powder X-ray diffraction data.

In this paper we wish to report the synthesis and the structural characterization of tin niobates $Sn_{1+x}Nb_2O_{6+x}$, $x = 0.0$, 0.5, and 1.0. The materials have been characterized by bulk chemical analysis, single-crystal and powder X-ray diffraction, and ^{119}Sn Mössbauer and ^{93}Nb and ^{119}Sn solid-state NMR spectroscopies. The samples have also been routinely characterized by SEM, EDS, and Raman spectroscopy but these results will not be presented here.

EXPERIMENTAL

Samples. Tin niobates ($Sn_{1+x}Nb_2O_{6+x}$, $x = 0.0$, 0.5, and 1.0) have been prepared by both mixing of the oxide precursors and by the so-called flux method (8). In the former, stoichiometric amounts of SnO (Aldrich, 99%) and Nb_2O_5 (Aldrich, 99.9%) have been ground and carefully mixed in an agate mortar. This mixture has been enclosed in quartz ampoules, sealed under vacuum, calcined at 900°C (heating rate 2°C/min), kept at this temperature for 4 h, and cooled down to room temperature. The sample with $x = 2$ has been prepared by this method and labeled $Sn_2Nb_2O_7$ (1). The sample labeled as $Sn_2Nb_2O_7$ (2) has been prepared by the flux method using NaCl (Merck, p.a.) with an excess
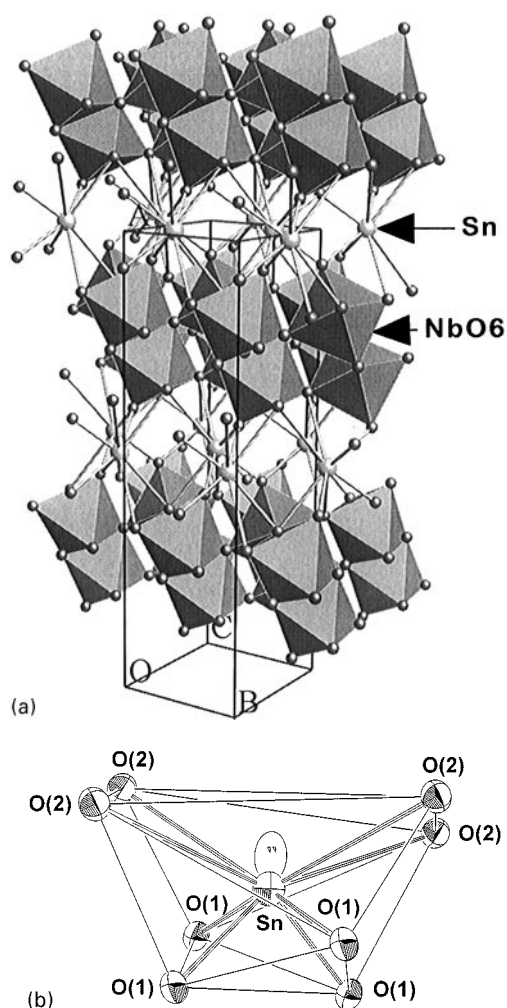
FIG. 1. (a) Schematic view of the foordite structure; (b) stereoactive Sn(II) lone pair in foordite.

of $SnCl_2$ (Aldrich, 99.9%) relative to $NaNbO_3$ (Aldrich). This mixture has been enclosed in a quartz ampoule, sealed under vacuum, and calcined at 1100°C (heating rate 2°C/min) and kept at this temperature for 10 h.

Techniques. Powder X-ray diffraction (XRD) patterns have been recorded on a X'Pert MPD diffractometer using $CuK\alpha$ radiation. A suitable red octahedral single crystal (size $0.02 \times 0.02 \times 0.02$ mm) of $Sn_2Nb_2O_7$ (2) has been examined by single-crystal X-ray diffraction on a Nonius Kappa CCD instrument. Experimental details are given elswhere (9).

[119]Sn Mössbauer spectra were recorded in the constant acceleration mode by transmission on a conventional spectrometer. The γ source was [119]Sn in $BaSO_4$ matrix. The velocity scale was calibrated with the magnetic sextet on a high purity iron foil absorber, using [57]Co(Rh) as source. The absorbers were prepared to have 1–2 mg of [119]Sn per

cm[2]. Recorded spectra were fitted with Lorentzian profiles by a least-squares method. The origin of the isomer shift was determined from the center of the $BaSnO_3$ room-temperature spectrum.

[93]Nb and ^{119}Sn solid-state NMR spectra have been recorded at 97.84 and 149.09 MHz, respectively, on a Bruker MSL 400P spectrometer. [93]Nb magic-angle spinning (MAS) NMR spectra have been recorded on a 2.5-mm Bruker double-bearing probe using a spinning rate of 32 kHz, a 0.6-μs (equivalent to ca. 7°) pulse, and a 0.5-s recycle delay. Static [93]Nb spectra have been acquired on a Bruker probe using a 9°-τ-90°-τ-acq. echo sequence, with a τ value of 50 μs. The length of the first pulse has been chosen in order to obtain an almost undistorted spectral line. ^{119}Sn solid-state MAS NMR spectra have been recorded on a 4-mm double-bearing Bruker probe with a spinning rate of 14 kHz, a 3-μs (equivalent to ca. 50° pulse) and a 30-s recycle delay. All spectral simulations have been carried out using program QUASAR (10). Bulk chemical analysis by ICP has been carried out on a Jobin Yvon JY plus spectrometer.

RESULTS AND DISCUSSION

The powder XRD pattern of yellow $SnNb_2O_6$ (not shown), may be indexed as foordite with $a = 17.11$ Å. As-prepared $Sn_2Nb_2O_7$ (2) contains both yellow acicular crystals and red octahedral crystals, which are easily separated from each other. The powder XRD pattern of the yellow crystals may be indexed assuming a tetragonal tungsten bronze (11) lattice with $a = 12.385(1)$, $c = 3.9170(6)$ Å. The single-crystal XRD pattern of the red crystals may be indexed as a pyrochlore lattice with $a = 10.5386(5)$ Å. $Sn_{1.5}Nb_2O_{6.5}$ is a mixture containing synthetic foordite and $Sn_2Nb_2O_7$. Assuming a formula $Sn_{1+x}Nb_2O_{6+x}$, chemical analysis allows the determination of the tin content. The results are given in Table 1.

The structure of a red $Sn_2Nb_2O_7$ (2) crystal has been solved by single-crystal XRD. The extinction conditions confirm that the lattice is cubic type F. However, the study of the $0kl$ reflections is difficult because the reflections with $k + 1 \neq 4n$ have an intensity $I \approx 3\sigma_{(I)}$. If these reflections are considered as extinct, the space group is Fd-$3m$, the typical space group for pyrochlores. Otherwise, the space group is non-centrosymmetric $F4_132$. Birchall and Sleight have shown that their $Sn_2Nb_2O_7$ samples were indeed

TABLE 1
Chemical Analysis of $Sn_{1+x}Nb_2O_{6+x}$

$SnO:Nb_2O_5$	x	% Sn (m/m)	% Nb (m/m)
1:1	1	19.8	31.6
1.5:1	1.5	36.4	40.2
2:1 (1)	2	36.1	29.8

TABLE 2
Refinement Results of Single-Crystal $Sn_2Nb_2O_7$ (2)

Space group	N_{obs}	N_{param}	N_{ext} violation	R	R_w	
$F4_132$*	212	18	—	0.039	0.109	1.50
Fd-$3m$	150	18	1	0.022	0.062	1.27

Note. N_{obs}, number of unique observations; N_{param}, number of parameters; N_{ext}, number of violations of extinction $0klk + l = 4n$. The absolute configuration has been tested and the Flack parameter of the given solution is equal to 0.36(31).

TABLE 3
Selected Geometric Parameters (Å,°) of $Sn_2Nb_2O_7$ (2)

Nb1–O1^i	1.9811(10)	Sn1–O1^{iv}	2.730(5)
Sn1–O2^{ii}	2.311(4)	Sn1–O1^v	3.026(5)
Sn1–O1^{iii}	2.406(19)		
O1^{vi}–Nb1–O1^{vii}	90.59(11)	O2^{ii}–Sn1–O1^{iii}	106.3(5)
O1^{vi}–Nb1–O1^{viii}	89.42(11)	O2^{ix}–Sn1–O1^{iii}	88.2(4)
O2^{ii}–Sn1–O2^{ix}	162.2(11)	O1^{iii}–Sn1–O1^x	70.8(6)

Note. Symmetry codes: (i) $\frac{1}{4} - y, \frac{1}{4} - x, z$; (ii) $\frac{1}{2} - x, \frac{1}{2} - y, -z$; (iii) $y - \frac{1}{4}, \frac{1}{2} - z, x - \frac{3}{4}$; (iv) $-z, \frac{1}{4} + y, x - \frac{3}{4}$; (v) $\frac{1}{4} + y, -z, \frac{1}{4} + x$; (vi) $x - \frac{1}{4}, -z, y - \frac{1}{4}$; (vii) $y - \frac{1}{4}, x - \frac{1}{4}, -z$; (viii) $\frac{1}{4} - y, z, \frac{1}{4} - x$; (ix) $x - \frac{1}{2}, y, z - \frac{1}{2}$; (x) $\frac{1}{4} - y, \frac{3}{4} - x, z - \frac{1}{2}$.

noncentrosymmetric (7). We note, however, that their microcrystalline powders were yellow while our single crystals are red. We have decided to refine the structure considering both space groups. In the two cases, 18 atomic parameters have been refined, including the occupation factors of the atomic sites. In order to avoid the correlation between the thermal displacement parameters and the occupation factors, two constraints have been imposed to the latter: full occupation of the niobium site by both niobium and tin (IV) and electroneutrality of the compound. It has been found that the R and R_w agreement factors were better for the refinement in the centrosymmetric space group Fd-

$3m$ (Table 2). The two refinements yield the same lacunar pyrochlore formula for red $Sn_2Nb_2O_7$ (2) (9): $Sn_{1.34}Nb_{1.68}Sn_{0.32}O_{6.18}$. Group Fd-$3m$ has, thus, been chosen. Tin has been located in two different sites (Fig. 2). The first ($16c$) site is shared by both niobium and tin. The second ($96h$) site is located away from the axis of the tunnels and between the centres of the two adjacent cavities. The environment of tin in this site is distorted (Fig. 2b), with six oxygen neighbors, corresponding to the NbO_6 oxygens, plus two other oxygen atoms located at the cavities center (site $8b$), the classic O′ site for a pyrochlore $A_2B_2O_6O′$. Selected interatomic distances and angles are given in Table 3.

The ^{119}Sn Mössbauer spectroscopic data (Table 4) show that $Sn_2Nb_2O_7$ (1) contains both Sn(II) and Sn(IV). The structural determination of this solid yields the formula $Sn_{1.18}Nb_{1.63}Sn_{0.37}O_6$. The niobium site can accept only ions whose radii are close to that of Nb(V), 0.70 Å. On the other hand, ^{119}Sn Mössbauer spectroscopy indicates that 27% of tin is present as Sn(IV). Hence, it is likely that Sn(IV) (ionic radius 0.71 Å) occupies the niobium site. The reasons for the oxidation of Sn(II) to Sn(IV) are, at present, not entirely clear. In any case, some degree of oxidation seems to

FIG. 2. (a) Schematic view of the pyrochlore structure; (b) stereoactive Sn(II) lone pair in pyrochlore.

TABLE 4
^{119}Sn Mössbauer Data on $Sn_{1+x}Nb_2O_{6+x}$ Compounds

	Isomer shift (mm/s)	Quadrupole splitting (mm/s)	Molar %
$Sn_{1.5}Nb_2O_{6.5}$			
Sn (IV)	0.022(6)	0	13.3
Sn (II) (doublet 1)	3.42(2)	1.58(2)	65.1
Sn (II) (doublet 2)	3.10(2)	1.67(2)	21.5
Total Sn (II)			86.6
$Sn_2Nb_2O_7$ (1)			
Sn (IV)	0.037(2)	0	27.1
Sn (II) (doublet 1)	3.73(3)	1.56(3)	46
Sn (II) (doublet 2)	3.33(2)	2.04(2)	26.8
Total Sn (II)			72.9

$Sn_{1+x}Nb_2O_{6+x}$ Formulae Derived from Chemical Analysis and Mössbauer Spectroscopy

$SnO:Nb_2O_5$	Formula	$\%Sn^{IV}$
1:1	$Sn_{1.00}^{II}Nb_{2.01}O_6$	0
1.5:1	$Sn_{1.10}^{II}Nb_{1.81}Sn_{0.19}^{IV}O_6{}^a$	14.72
2:1 (1)	$Sn_{1.18}^{II}Nb_{1.63}Sn_{0.37}^{IV}O_6$	23.63

^{a} Average formula.

occur when the reactants are being ground in the agate mortar.

The pyrochlore formula must be modified in order to take into account the tin oxidation and the presence of Sn(IV) in the site of niobium. If 'a' is the relative amount of Sn(IV), then the pyrochlore formula $Sn_{1+x}Nb_2O_{6+x}$ may be written as $Sn_{(1+x)(1-a)}$ $(Sn_{(1+x)a}$ $Nb_2)O_{6+x+a(1+x)}$. Now, in the pyrochlore structure the formulae AB_2O_6 or $A_2B_2O_7$ only consider two B atoms. Thus, we may write the formula $Sn_{(1+x)(1-a)}^{II}$ $(Sn_{(1+x)a}^{IV}$ $Nb_{2-(1+x)a})O_{6+x-3a(1+x)/2}$, with $0 \leq x \leq 1$; $0 \leq a \leq 1$; $0 \leq x - 3a(1+x)/2 \leq 1$. It is now possible to calculate the mass percentage for the various elements,

$$\%Sn = (1+x)m_{Sn}/M$$

$$\%Nb = [2 - (1+x)a]m_{Nb}/M,$$

where M is the mass of the unit formula; that is, $M = (1+x)m_{Sn} + [2 - (1+x)a]m_{Nb} + [6 + x - 3a(1+x)/2]m_O$.

The use of these equations and the chemical analysis data leads to the formulae in Table 5 which agree well with the ^{119}Sn Mössbauer data. While sample $Sn_{1.5}Nb_2O_{6.5}$ is a mixture its average chemical formula is, nevertheless, in good agreement with the ^{119}Sn Mössbauer.

The ^{119}Sn Mössbauer spectra of the tin niobates studied (Fig. 3) consist of up to three well resolved peaks which can be analyzed in terms of two doublets, with isomer shifts characteristic of Sn(II) species, and a singlet ascribed to a Sn(IV) species. The quadrupole splittings contain information on the relative distributions of the $5p$ electron densities over all tin bonds and its lone electron pair. The factors influencing the isomer shift include the percentage of s character of the tin lone electron pair (12, 13). The isomer shift of the singlet is only slightly different from that of SnO_2 and indicates that Sn(IV) is in a fairly regular octahedral site with all six Sn–O distances equal or nearly so. In other words, Sn(IV) resides in the niobium site. The quadrupole splittings may be deconvoluted into two overlapping doublets. This shows that Sn(II) occupies two different and, in view of the quadrupole splittings, low symmetry sites in the structure. The fact that a single Sn(II) site has been found by XRD does not contradict this conclusion. Indeed, the local environment of tin in this site consists of $6 + 2$ oxygen
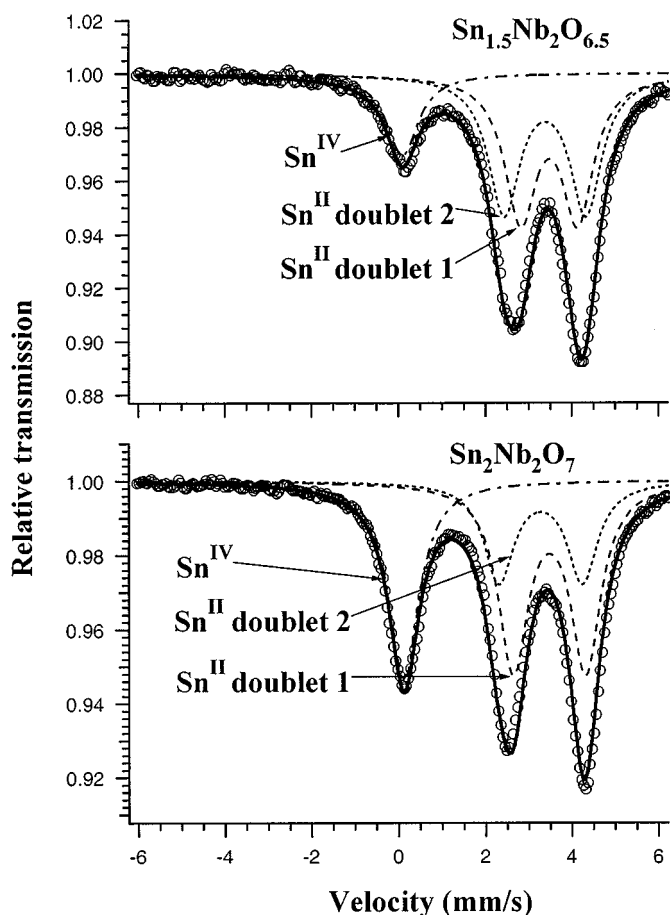
FIG. 3. ^{119}Sn Mössbauer spectra of $Sn_{1.5}Nb_2O_{6.5}$ and $Sn_2Nb_2O_7(1)$.

neighbors. However, because the samples are nonstoichiometric this environment really consists of both 6 oxygen neighbors and $6 + 2$ oxygen neighbors and, thus, there are two types of environments for Sn(II). These results are similar to those previously reported (7).
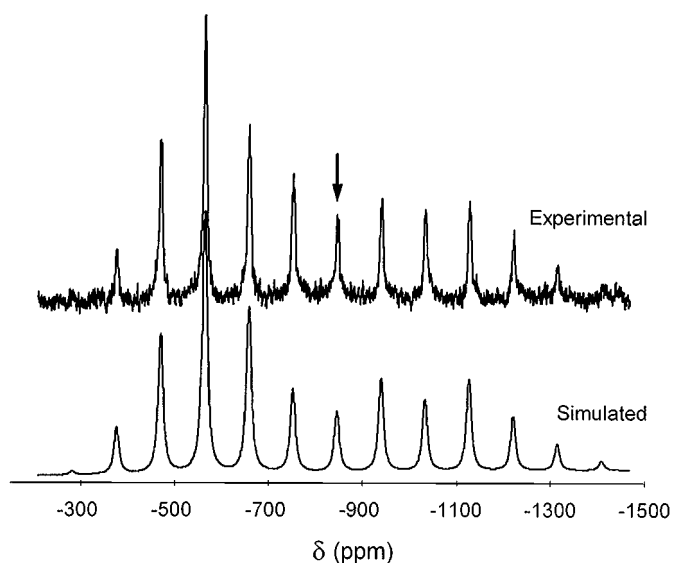
Pyrochlore-type compounds such as $A_2^{III}Sn_2^{IV}O_7$ (A^{III} is a rare-earth ion) are known to give ^{119}Sn Mössbauer spectra in which the resonance due to Sn(IV) is considerably broadened, indicating a distorted site (14). No such brodening has been observed for our compounds or for $Sn_{1.76}^{II}Ta_{1.56}Sn_{0.44}^{IV}O_{6.54}$.[7] For the latter, such observation has been attributed to the fact that O–Sn(IV)–O angles are close to $90°$. This is also the case for our sample $Sn_{1.34}^{II}(Nb_{1.68}Sn_{0.32}^{IV})O_{6.18}$ (Table 6). A number of Sn^{II}–O systems with known structures have been studied by ^{119}Sn Mössbauer spectroscopy (15, 16). For compounds in which the lone electron pair is stereoactive, the isomer shift ranges from 2.40 to 4.20 mm/s, relative to $BaSnO_3$ (14). The isomer shifts we have measured fall in this range, indicating that the s electron density has a similar percentage of s character in the Sn–O bonds as found in other tin(II) oxides. The

TABLE 6
Distances and Angles of $Sn_2Nb_2O_7$ (2) (Å, °)

	$Fd\text{-}3m$	$F4_132$
Nb1(Sn2)–O1	1.9811(10)	1.980(2)
Sn1–O1	2.406(19)	2.421(4)
Sn1–O2	2.311(4)	2.3063
O1–Nb1–O1	90.59(11)	90.48(12)
	89.42(11)	89.52(12)
O2–Sn1–O2	162.2(11)	163.06(16)
O2–Sn1–O1	88.2(4)	87.83(7)
	106.3(5)	106.18(9)
O1–Sn1–O1	70.8(6)	70.30(9)

FIG. 5. ^{119}Sn MAS NMR spectrum of $Sn_2Nb_2O_7$(1).

relatively large quadrupole splittings measured are expected when the lone electron pair is stereoactive (12).

The ^{119}Sn MAS NMR spectra of $SnNb_2O_6$ and $Sn_2Nb_2O_7$ (1) are shown in Figs. 4 and 5. The former displays an isotropic peak at -751 ppm and large number of spinning sidebands, indicating a relatively large chemical shift anisotropy (CSA $= -929$ ppm, $\eta = 0.15$). $Sn_2Nb_2O_7$ (1) gives a single, very broad resonance (full width at half-maximum, FWHM $= 8.0$ kHz) centered at about -605 ppm [not enough sample was available to record a spectrum of $Sn_2Nb_2O_7$ (2)]. Most systematic ^{119}Sn MAS NMR studies have been concerned with organotin compounds (17) and a few tin oxides (18–21). Mundus et al. have shown that the isotropic chemical shift allows to distinguish between different coordination numbers of Sn(IV) present in tin sulfides (22). For example, four-coordinated tin in $Na_6Sn_2S_7$ resonates at 61.7 ppm while six-coordinated tin in Na_2SnS_3 and SnO_2 give peaks at, respectively, -773.1

and -603 ppm (21, 22). On the other hand, six-coordinated Sn(II) in SnS resonates at -300 ppm. Four-coordinated tin in SnO gives a peak at -208 ppm (21) while eight-coordinated Sn(II) in $Sn_2P_2S_6$ resonates at -754.5 ppm (23). Foordite ($SnNb_2O_6$) contains $Sn^{II}O_8$ antiprisms and, thus, the -751 ppm ^{119}Sn isotropic chemical shift observed for synthetic foordite is consistent with this coordination. The relatively large chemical shift anisotropy (-929 ppm) confirms the large distortion of the local tin environment. As shown by ^{119}Sn Mössbauer spectroscopy, $Sn_2Nb_2O_7$ (1) contains both six-coordinated Sn(IV) and eight-coordinated Sn(II). Now, the ^{119}Sn isotropic chemical shift data available strongly suggests that these two tin environments may resonate approximately in the same spectral region. In addition, the local environment of Sn(II) in $Sn_2Nb_2O_7$ is disordered and this gives rise to a distribution of chemical shifts which broadens the spectral lines. In other words, it may not be possible to distinguish by ^{119}Sn MAS NMR six-coordinated Sn(IV) from eight-coordinated Sn(II) (particularly when it is not possible to record spectra with very good signal-to-noise ratios). One question remains
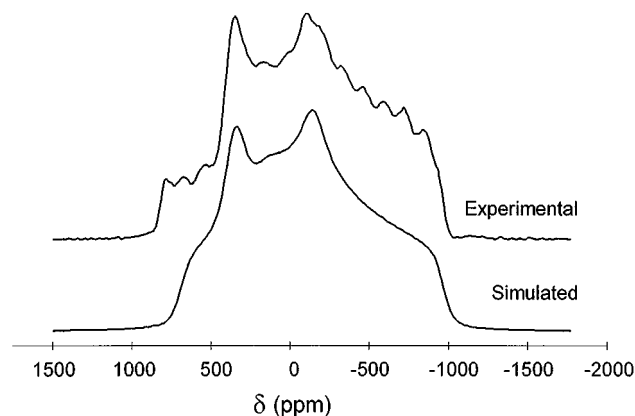

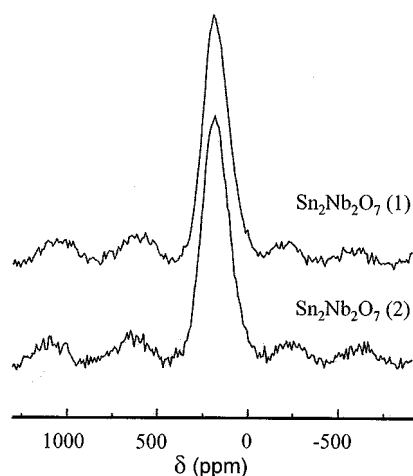**FIG. 4.** Experimental and simulated ^{119}Sn MAS NMR spectra of synthetic foordite. The arrow depicts the isotropic peak.

FIG. 6. Experimental and simulated static ^{93}Nb NMR of synthetic foordite.

FIG. 7. ^{93}Nb MAS NMR spectra of $Sn_2Nb_2O_7$(1), (2).

unanswered: even if in the ^{119}Sn MAS NMR spectrum of $Sn_2Nb_2O_7$ (1) the Sn(II) and Sn(IV) isotropic lines overlap we should still expect to observe strong spinning side bands from the distorted Sn(II) sites. Such side bands are, however, not seen.

The static ^{93}Nb spectrum of $SnNb_2O_6$ (Fig. 6) displays a very broad second-order quadrupole powder pattern which can be simulated yielding an isotropic chemical shift of 140 ± 5 ppm, a very large quadrupole coupling constant $C_Q = 38 \pm 1$ MHz and an asymmetry parameter of 0.6 ± 0.2. The large C_Q value is consistent with a fairly distorted local environment for niobium. Indeed, in the structure of foordite the Nb–O distances in the NbO_6 octahedron range from 1.85 to 2.16 Å. The ^{93}Nb MAS NMR spectra of the $Sn_2Nb_2O_7$ (1), (2) samples display much sharper (FWHM 10.7 kHz), almost symmetric, peaks at 190 ppm (Fig. 7) indicating a relatively symmetric octahedral environment for niobium, in accord with the crystal structure of $Sn_2Nb_2O_7$ (2).

REFERENCES

1. W. R. Cook and H. Jaffe, *Phys. Rev.* **88,** 1426 (1952).
2. W. R. Cook and H. Jaffe, *Phys. Rev.* **88,** 1297 (1953).
3. J. Galy, G. Meunier, S. Andersson, and Å. Astrom, *J. Solid State Chem.* **13,** 142 (1975).
4. K. Sreedhar and A. Mitra, *J. Am. Ceram. Soc.* **82,** 1070 (1999).
5. P. Cerny, A.-M. Fransolet, T. S. Ercit, and R. Chapman, *Can. Mineral.* **26,** 889 (1988).
6. T. S. Ercit and P. Cerny, *Can. Mineral.* **26,** 899 (1988).
7. T. Birchall and A. W. Sleigth, *J. Solid State Chem.* **13,** 118 (1975).
8. W. Tang, H. Kanoh, and K. Ooi, *Electro. Solid-State Lett.* **3,** 145 (1998).
9. L. P.Cruz, J. M. Savariault, and J. Rocha, submitted for publication.
10. J. P. Amoureux, C. Fernandez, L. Carpentier, and E. Cochon, *Phys. Status Solidi A* **132,** 462 (1992).
11. S. I. Ijima and J. G. Allpress, *Acta Crystallogr. A* **30,** 22 (1974).
12. E. Hough and D. G. Nicholson, *J. Chem. Soc. Dalton Trans.* 2083 (1981).
13. N. N. Greenwood and T. C. Gibb, "Mössbauer Spectroscopy." Chapman and Hall, London, 1971.
14. L. M. Belgaev, I. S. Lyubutin, L. N. Dem'yanets, T. V. Donitrieva, and L. P. Mitina, *Soviet Phys. Solid State* **11,** 424 (1969).
15. C. C. Davies and J. D. Donaldson, *J. Chem. Soc. A* 424 (1968).
16. J. D. Donaldson, D. G. Nickolson, and B. J. Saniar, *J. Chem. Soc. A* 946 (1968).
17. A. Sebald, *in* "NMR Basic Principles and Progress," Vol. 31, p. 91 Springer Verlag, Berlin, Heidelberg, 1995.
18. A. K. Cheetham, C. M. Dobson, C. P. Grey, and R. J. B. Jakeman, *Nature* **328,** 706 (1987).
19. C. P. Grey, C. M. Dobson, A. K. Cheetham, and R. J. B. Jakeman, *J. Am. Chem. Soc.* **111,** 505 (1989).
20. N. J. Clayden, C. M. Dobson, and A. Fern, *J. Chem. Soc. Dalton Trans.* 843 (1989).
21. C. Cossement, J. Darville, J.-M. Gilles, J. B. Nagy, C. Fernadez, and J. -P. Amoureux, *Magn. Reson. Chem.* **30,** 263 (1992).
22. C. Mundus, G. Taillades, A. Pradel, and M. Ribes, *Solid State NMR* **7,** 141 (1996).
23. D. C. Apperley and R. K. Harris, *Chem. Mater.* **5,** 1772 (1993).